Performance analysis of friction surfacing between two dissimilar materials

Dillip Kumar Sahoo
Asst. professor, Dept. of Automobile Engineering,
Sathyabama University, Chennai

Bhulok Sundar Mohanty
Professor, Dept. of Mechanical Engineering,
Eswari Engineering College, Chennai

Abstract: This work reports on the performance analysis of deposition of copper on mild steel using friction surfacing method. Commercial mild steel was chosen as the substrate and commercial pure copper as the consumable rod. Performance criteria were tested in the friction surfacing of mild steel, for a range of process parameters including forging force, consumable tilt angle, travel and rotation speeds. The applied load on the consumable rod was found to be essential to improve joining efficiency and to increase the deposition rate. Higher rotation or travel speeds were detrimental for the connection potency .Tilting the expendable rod on the travel direction proved to improve the joining efficiency up to 5%.The unbonded regions were reduced to 9 % of the effective coating section. Friction surfacing was seen to need mechanical work between 2.5 and 4 kJ/g of deposited coating with deposition rates of 0.4–1.5 g/s.
Keywords: mild steel, cupper, forging force, tilt angle, rotational speed, friction surfacing.

I. INTRODUCTION

Friction surfacing is a solid section protection technique that uses a mix of heat and deformation to clean surfaces and metallurgically bonded metals. In its simplest arrangement, a rotating expendable bar is brought into contact, beneath low load, with stationary substrate in the initial dwell time stage, as shown in Fig. 1, when the rotating bar is preferentially heated by the frictional heat development because of relative motion between the rotating expendable rod and stationary substrate, facilitating to the consumable to plastic state. After the dwell time, the substrate that's mounted on a table is given linear translational motion to facilitate the deposition of the plasticized consumable onto the substrate by shearing. Bonding occurs by the combination of self cleansing between the two materials and also the application of heat and pressure to promote diffusion across the interface, thereby forming a solid-phase metallurgical bond. The process depends on manufacturing exactly the correct temperature and shear conditions at the interface between the rotating bar and substrate via the plasticized layer

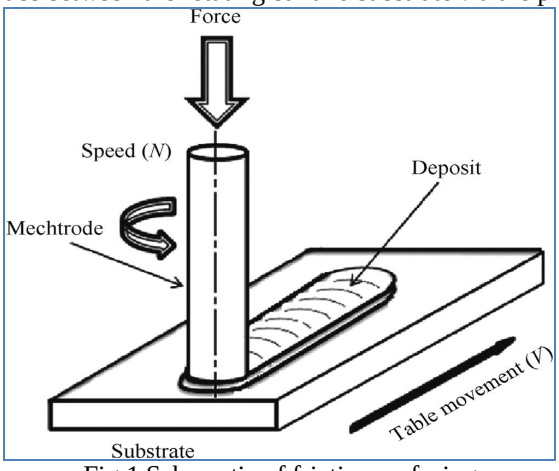

Fig.1.Schematic of friction surfacing

Friction surfacing permits to deposit numerous dissimilar material combinations. Rafi et al. (2011), Batchelor et al. (1996) and Chandrasekaran et al. (1997) investigated the deposition of stainless steel, tool steel and nickelbased alloys (Inconel) on mild steel substrates, as well as, stainless steel, mild steel and inconel consumables on aluminium substrates. Friction surfacing was additionally used to manufacture aluminium metal matrix composites on aluminium and titanium substrates by Reddy et al. (2009, 2011).

According to Macedo et al. (2010), friction surfacing has been employed in the production of long life industrial blades, wear resistant elements, anticorrosion coatings and in the rehabilitation of worn or damaged parts such as, turbine blade tips and agricultural machinery. alternative applications feature the hard facing of valve seats with stellite and tools such as punches and drills.

The influence of process parameters on deposit characteristics and bonding strength was addressed. Vitanov et al. (2000) developed a decision support system to correlate the resulting bond strength, coating thickness and dimension with forging force, spindle and travel speeds. the increase of forging force improved the bond strength and reduced the coating thickness. The undercut region was reduced at higher formation forces and enhanced at quicker travel speeds.Vitanov et al. (2010) observed that higher ratios between the feed rate of the consumable and the travel speed resulted in superior bonding quality, as well as, lower to intermediate values of rotation speed. In the friction surfacing of low carbon steel with tool steel H13 consumables, Rafi et al. (2010) concluded that the coating dimension was powerfully influenced by the rotation speed, while thickness was mostly determined by the travel speed.

Since the deposition results from severe viscoplastic deformation, friction surfacing presents some advantages over other coating technologies based on fusion welding or heat spraying processes, that manufacture coarse microstructures and cause intermetallics formation, thereby deteriorating the mechanical strength of the coatings. Other techniques can prevent this problem as shown by Lachenicht et al. (2011) using spray forming. Macedo et al. (2010) expressed that except avoiding defects commonly associated to fusion and solidification mechanisms (porosities, hot cracking or slag inclusions), the heat input in friction surfacing is minimum and localized, preventing part distortion and minimizing the heat affected zone and dilution. Additionally, the absence of spatter, toxicant fumes and emission of radiation makes this method cleaner and environmentally friendly. However, friction surfacing currently struggles with several technical and productivity problems which contribute to a restricted vary of engineering applications. Further work is needed to develop friction surfacing as a competitive alternative to other existing coating technologies. Comparison between coating processes should think about the quantification of deposition rates and energy efficiency, which have not been determined for friction surfacing.
This paper aims to quantify the mass transfer rate in friction surfacing, contributing to establish a realistic comparison with other coating technologies and to present a deep study of the process parameters.

II. MATERIALS AND METHODS

Commercial pure Cu (CP Cu) was used as consumable rod. It was extruded from with diameter 18 mm and length 100 mm. The rod was held with the aid of a suitable collect n the spindle of a friction stir machine. The mild steel (MS) plate of 8 mm thickness, 100 mm width and 150 mm length was used as substrate. The substrate surface, on which friction surfacing would be done, was machined by using milling machine with stub arbor carbide face milling cutter. Friction surfacing was carried out using a horizontal friction stir welding machine. Substrate was held using strap clamps, just before surfacing; the surface of the substrate was cleaned by acetone to remove unwanted dust, dirt, oil, grease, etc.

Initially, a few trial experiments were done to narrow down the process parameters with a criterion of visible copper deposition. Following are the process parameters selected after initial trials. Rotational speed, rpm is varied as N= 1500, 2000 and 2500. Travel speed (γ, mm/s) is 4.1, 7.3 and 10.5 axial load KN is 2, 3 and 4 KN and tilt angle(α) is varied as 1,2 and 3 degree. In total, 9 samples were investigated and they are labelled as A, B, C.....I. They are listed in the Table 1. All the experiments were carried out in open atmosphere. Initial heating time of 90 seconds was kept constant for all the experiments. Runs were done across the substrate and were usually in the range of 20-40 mm. Verdict on the quality of the deposition is done visually ad commented as in table1. Morphology and composition of the deposit was studied using SEM and phase identification of deposit by XRD.

III. RESULTS AND DISCUSSION

3.1 Quality of deposition

Quality of the deposition is decided based on the visual examination. Deposits are classified as continuous, uniform, non uniform, gradually increasing width, varying width, shearing deposit, narrow deposits, etc. Continuous and uniform deposits are achieved only for certain combination of travel speed and rotational speed as shown in table 1. the consumable tool was clearly bad in the case of C and I through the deposit appearance is good, the tool is bad in the case of F. the roughness of the deposits is measured and they are in the range of 0.5 μm to 4.1μm.

Sample No	Force (KN)	N(rpm)	Travel speed(mm/sec)	Tilt angle(degree)	Comment
A	2	1500	4.1	1	Continuous, uniform width, satisfactory deposition
B	2	2000	4.1	1	Continuous, gradually increasing width
C	2	2500	4.1	1	Discontinuous, non uniform and shearing deposition
D	3	1500	7.3	2	Uniform and continuous deposition
E	3	2000	7.3	2	Continuous and good deposition, bonding width slightly increases
F	3	2500	7.3	2	Continuous good deposition and varying bonding width.
G	4	1500	10.5	3	Non uniform, varying width and shearing deposition at the end
H	4	2000	10.5	3	Non uniform, continuous deposition, thickness increasing
I	4	2500	10.5	3	Non uniform, width and thickness of the bonding increases

3.2 Metallurgical analysis

Fig. 2 presents a cross section macrograph of each rod and coating, depiction the gradual transformations of the consumable material into the deposit as it is plunged downwards. The fitting between the surfaces of the expendable and also the coating will be determined, as well as, the flash developed. it depicts the gradual transformations that the tool has undergone as it deposited on the substrate. The consumable rod has a coarse equiaxed grain structure, initially as shown in Fig 2a. The hot working of the consumable rod tip and the deposit generates heat which is conducted along the consumable, preheating the material and enabling its plastic deformation. Thus, heat conducted into the consumable is not considered as an energy loss, since it preheats the consumable material that will be processed into coating.

Fig. 2b depicts the heat affected microstructures because of the temperature increase which, by promoting diffusion. Evidences of plastic deformation can be seen in Fig. 2c. Since the heat exposed material was softened and extruded by the colder material layers higher than. the combination of plastic deformation and heat generation results into dynamic recrystallization (Fig. 2d).

Since the hot deposit of viscoplastic material is pressed against the substrate at temperatures about 70% of the melting point, a diffusion bonding process takes place. Plastic deformation and friction can disrupt the comparatively brittle oxide layers, establishing metal to metal contact enabling the joining process.

Heat is lost mainly by conduction to the substrate, originating in a heat affected zone, almost like the consumable. Heat affected zones at the substrate and the consumable are characterized by a hardness increase (Fig. 2f).

Fig. 3 illustrates a proposed model for the world thermal and mechanical processes concerned during friction surfacing, based on the metallurgical transformations described above.

The speed difference between the viscoplastic material, which is rotating along side the rod at vxy, and also the material effectively joined to the substrate ($vxy = 0$), causes the deposit to detach from the consumable. This viscous shearing friction between the deposit and also the consumable is that the most important heat supply in the process.

Since the deposited material at the lower end is pressed without lateral confinement, it flows outside the consumable diameter, resulting into a revolving flash attached to the tip of the consumable rod and side boundless regions adjacent to the deposit. Flash and unbonded regions play an important role as boundary conditions of temperature and pressure for the joining process.

By suddenly extracting the expendable throughout the deposition stage (stop action procedure) it is possible to analyze instantaneously the process. Fig. 5 suggests that the material is not transferred strictly on a vertical direction, as there's a contribution from rotation speed, travel speed and tilt angle. Plastic deformation of the substrate evidences that the consumable material is rubbed against it from the advancing to the retreating aspect, totally bonding at the back of the rod from the retreating to the advancing side.

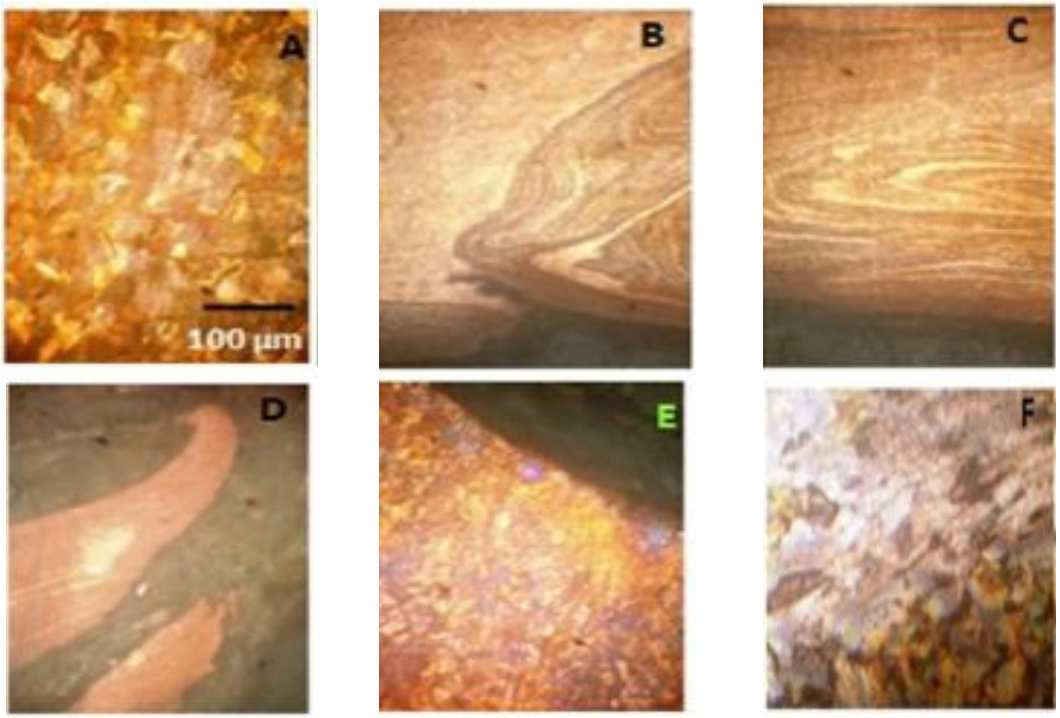

Fig. 2. Microstructural transformations during friction surfacing. (a) Consumable base material, (b) heat affected zone, (c) thermomechanically affected zone, (d) full recrystallized microstructure, (e) coating microstructure and (f) heat affected substrate. Process parameters: F = 3 kN; Ω = 2500 rpm; *v* = 7.3 mm/s.

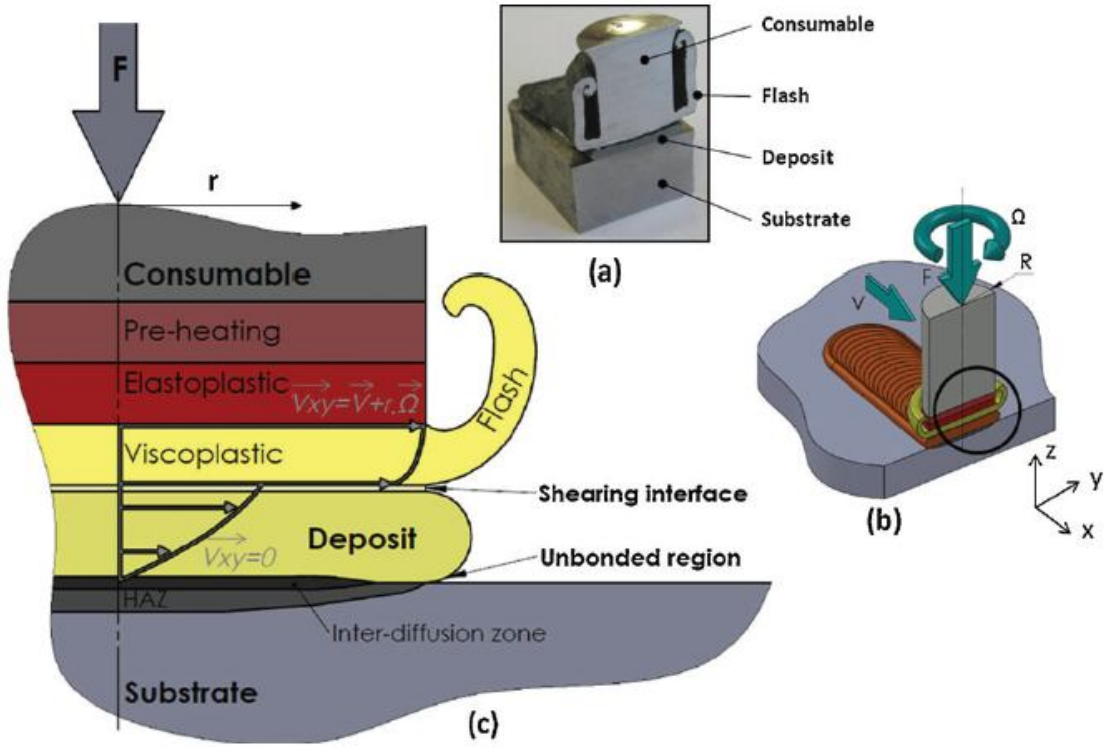

Fig. 3. Thermomechanics of friction surfacing. (a) Sectioned consumable, (b) process parameters and (c) thermomechanical transformations and speed profile. F – forging force; Ω – rotation speed; *v* – travel speed and Vxy – speed resultant in plan xy given by composition of rotation and travel speeds.

3.3. Influence of process parameters

3.3.1. Forging force

Increasing the forging force improves bonding and leads to wider and thinner deposits. However, excessive loads result in non uniform deposition with a depression at the middle of the pass due to material expelling from the region beyond consumable rod diameter. Table 1 depicts the effect of forging force on deposition, for a rotation speed of 2000 rpm and a travel speed of 4.1 mm/s. shows a poor deposition produced under a force of 2 kN.

3.3.2. Travel speed

Travel speed strongly influences coating thickness and width, as consumable travel speed across the substrate determines the speed at that material is deposited. As such, higher travel speeds result in thinner deposits. Fig. 4 depicts the influence of travel speed on coating microstructure. Faster travel speeds cause shorter heat exposure periods, leading to less grain growth and finer biotitic microstructures.

3.3.3. Rotation speed

Rotation speed was found to influence the bonding quality. Although the decrease from 2500 to 1500 rpm resulted in improved bonded width, higher rotation speeds produced a more flat and regular deposit, with a more effective forging effect shaping the coating.

3.3.4. Tilt angle

Tilting the consumable rod was seen to influence mainly the bonded width, as depicted in Fig. 6. Tilting the consumable rod from 0 to 3 degree increases the coating bonding width by about 09%. This can be justified by a more efficient confinement of viscoplastic material. Dimensional characterization presented in Fig. 6 is consistent with the macroscopic observations, showing the effect of forging force, tilt angle, rotation and travel speed on coating thickness, width and bonded width. For the testing conditions during this study, the deposits showed a

thickness varying between 0.7 and 2.2 mm and a width between 8.9 and 16.1 mm. Fig. 6d depicts the slight increase of bonded width for the increase of consumable rod tilt angle. Coating thickness and dimension don't seem to be considerably affected under the present test conditions. It can be concluded that the decrease in bonding width inherent to excessive travel and rotation speeds will be treated by adjusting a correct consumable rod tilt angle and forging force.

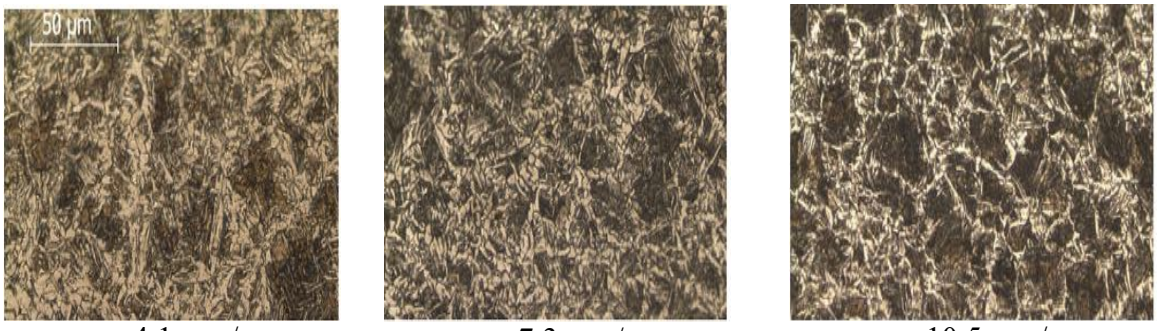

Fig. 4. Photomicrograph of coating cross section showing the effect of travel speed on coating microstructure. Process parameters: F = 3 kN, Ω = 2000 rpm.

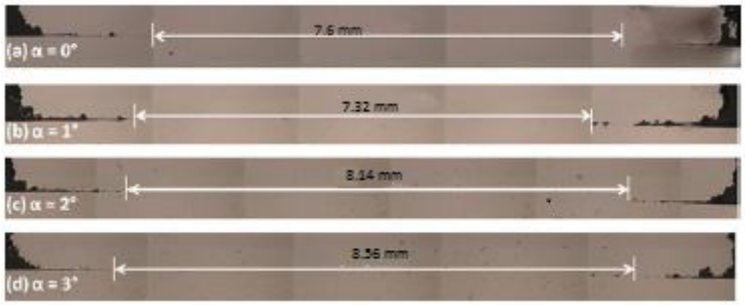

Fig. 5. Effect of tilt angle on bonding interface. Process parameters: F = 5 kN, Ω = 2500 rpm and *v* = 10.5 mm/s.

IV. PERFORMANCE ANALYSIS

In order to analyze the performance of friction surfacing, the following quantitative variables were defined to support an effective analysis of the material deposition and energy efficiency.

4.1. Mass transfer

Fig. 2 depicts the material flow from the consumable rod to the deposit bonded to the substrate. Volumetric rod consumption rate (CRvol) is determined by multiplying the rod plunging speed (Vz) by its cross section area (Ar), where r is the rod radius.

$$CRvol\ (m^3/s) = Ar.Vz = \pi r^2 Vz \quad (1)$$

Likewise, the product between the travel speed (*v*) and the deposited cross section area (Ad), expresses the volumetric deposition rate (DRvol) throughout the friction surfacing process (2).

$$DRvol\ (m^3/s) = A.dv \quad (2)$$

Considering the mild steel density (ρ), CR and DR can be rewritten in order to express the mass flow, as depicted by (3) and (4).

$$CR\ (kg/s) = CRvol \times \rho \quad (3)$$

$$DR\ (kg/s) = DRvol \times \rho \quad (4)$$

The consumable copper radius and mild steel density remain constant while *v* and Vz were measured by the data acquisition system during deposition. Cross section area was measured by image processing in cross section macrographs. Fig. 7 presents the deposition (DR) and consumption (CR) rates for the tested conditions. Deposition

rates were seen to vary from 0.5 to 1.5 g/s, increasing for higher forging forces, travel speeds and tilt angles. For higher rotation speeds, DR drops. Obviously the consumption rate is always higher than the deposition rate and closely follows its variation.

In order to determine the fraction of consumed material deposited and that transferred to flash, deposition efficiency (Ηefficiency) can be defined as the ratio between DR and CR, as follows:

$$\text{Ηdeposition} = \frac{DR}{CR} \quad (5)$$

However, due to the formation of side unbonded regions, just a part of the deposited material are effectively joined. As such, the joining efficiency (Ηjoining) is given by the ratio between the bonded width (Wb) and the maximum coating width (Wd), as shown schematically in Fig. 7.

$$\text{Ηjoining} = (Wb/Wd) \quad (6)$$

Thus effective coating efficiency (Ηcoating) reflects the fraction of consumed rod that is actually bonded to the substrate and is estimated by multiplying (5) and (6):

$$\text{Ηcoating} = \text{Ηdesposition} \cdot \text{Ηjoining} = (AdV/\pi r^2).(Wb/Wd) \quad (7)$$

Fig. 8 shows the effect of process parameters on the variables established above.

As shown in Fig. 8a, increasing the forging force significantly contributes to improve the coating efficiency, Ηcoating. as this load contributes to the improvement of bonded width and thus joining efficiency, Ηjoining. Material loss in flash formation seems to decrease when the forging force is in the range of 1–4 kN. However, the flash and undercut regions severely increased to provide enhanced forging closure. Fig. 8b depicts the improvement of deposition efficiency and loss of joining efficiency for higher travel speeds. Overall process mass transfer efficiency (Ηcoating) is not significantly affected by the travel speed.

The effect of rotation speed in coating process efficiency is mainly controlled by the joining efficiency.. The increase of rotation speed higher than 1500 rpm results in an increase of flash percentage, with consequent decrease in deposition efficiency, as shown in Fig. 8c. As shown in Fig. 8d, by adjusting the tilt angle, joining efficiency was slightly improved, resulting in a coating efficiency improvement of 4–9%. Process parameter optimization was capable of reducing the unbonded region to a minimum of 9%. Maximum joining efficiency and coating efficiency reached 70% and 45% respectively.

4.2. Energy consumption

The mechanical power supplied by the equipment (We) can be divided into three main contributions regarding rod rotation (Wr), axial plunging (Wz) and travel (Wx), as determined by (8)

$$We\ (J/s) = Wr + Wz + Wx = (2\pi\Omega/60)x\ (T_1 - T_0) + FzVz + Fxv \quad (8)$$

T_0 is the torque required to freely rotate the consumable rod without any contact friction e.g., the torque applied by the machine to impel the prescribed rotation speed and depends on the machine mechanical design, rather than deposition process. When the machine starts to plunge the rod against the plate substrate it raises the torque from T_0 to T_1.

Hence, for a joining efficiency of 100%, energy consumption per deposited unit of mass (specific energy consumption, SEC) as given by (9)

$$SEC\ (J/kg) = \dot{}(We/DR) \quad (9)$$

Fig.9 depicts the variation of power and specific energy consumption for the tested conditions. The power increases with the forging force and the travel speed. By increasing rotation speed from 1000 to 2500 rpm, the power drops approximately 45%.

Power consumption variation with process parameters seems to be consistent with joining efficiency. The equipment will have to exert additional mechanical power to impel the consumable if the resulting thermomechanical conditions improve bonding. Power consumption is strongly affected by the forging force and the rotation speed, varying between 2 and 4 kW.

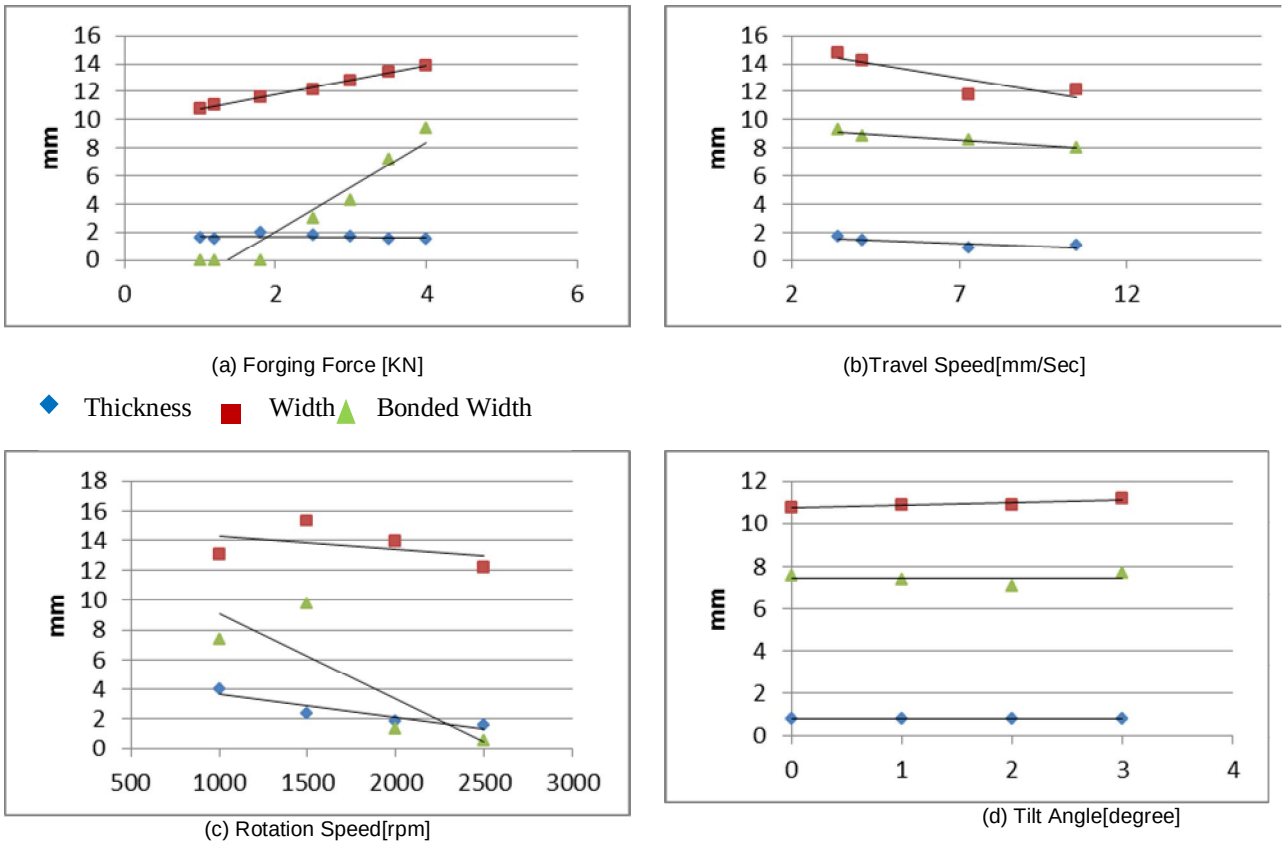

Fig.6. Effect of process parameter on coating thickness, width and bonded width. process parameters(a)Ω = 2000 rpm, γ=4.1 mm/sec (b) F= 3 KN, Ω = 2000 rpm(c) F= 2KN, γ=4.1 mm/sec (d) F= 3 KN, Ω = 2000 rpm, γ= 10.5 mm/sec

The specific energy consumption computed according to Eq. (9) varies from 2.5 to 4 kJ/g. Specific energy consumption increases with the forging force (Fig. 9a). Despite the increase in power specific energy consumption decreases with travel speed (Fig. 9b), given a more significant improvement of deposition rate (Fig. 8b). Hence, faster travel speeds allow to improve deposition rates whereas decreasing specific energy consumption. for high rotation speeds, though both the required power and the deposition rate drop, specific energy consumption rises, meaning that the decrease in deposition rate is more significant (Fig. 9c). Excessive rotation speeds result in less joining efficiency and increased specific energy consumption per unit of mass. By adjusting a correct tilt angle, specific energy consumption drops, whereas improving deposition rate and joining efficiency.

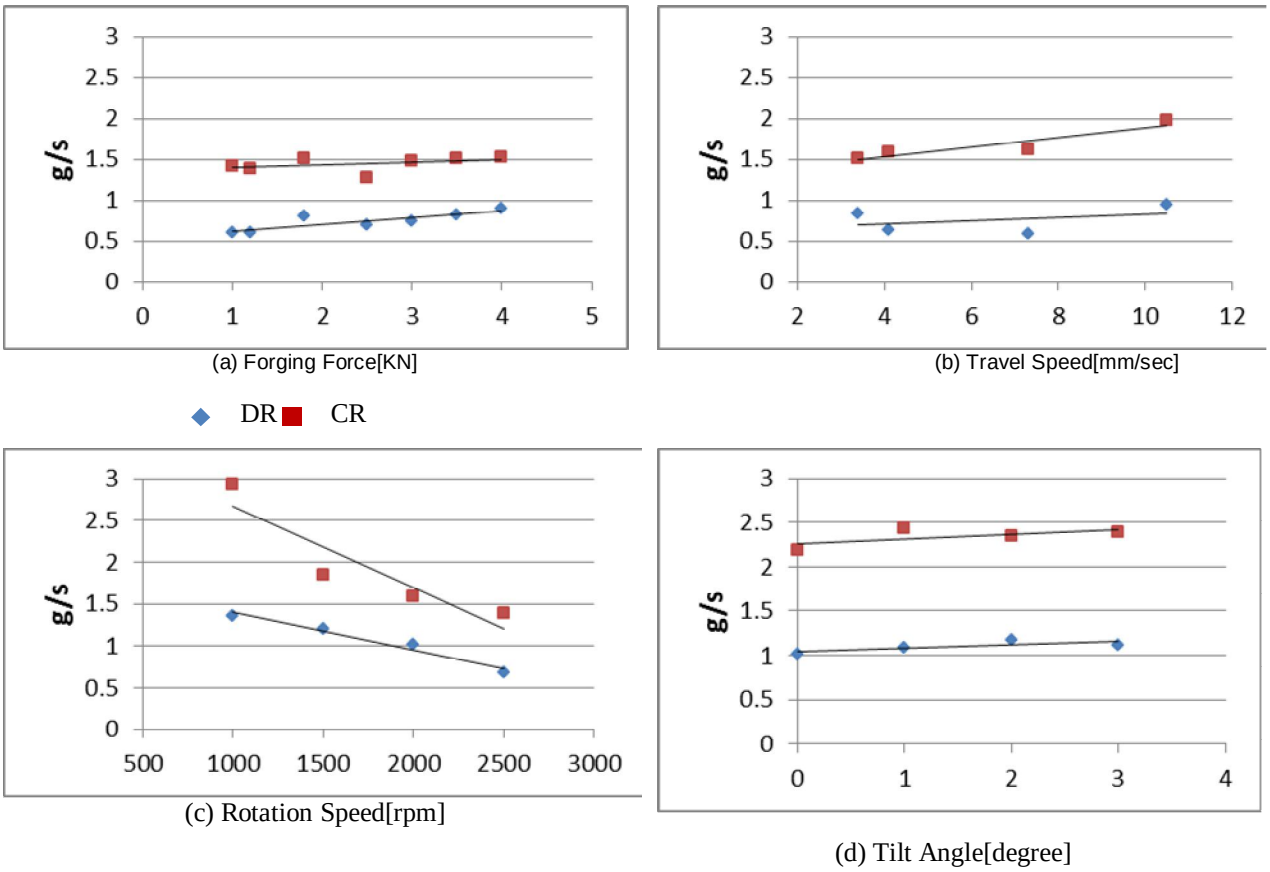

Fig.7. Effect of process parameter on coating thickness, width and bonded width. process parameters(a)Ω = 2000 rpm, γ=4.1 mm/sec (b) F= 3 KN, Ω = 2000 rpm(c) F= 2KN, γ=4.1 mm/sec (d) F= 3 KN, Ω = 2000 rpm, γ= 10.5 mm/sec

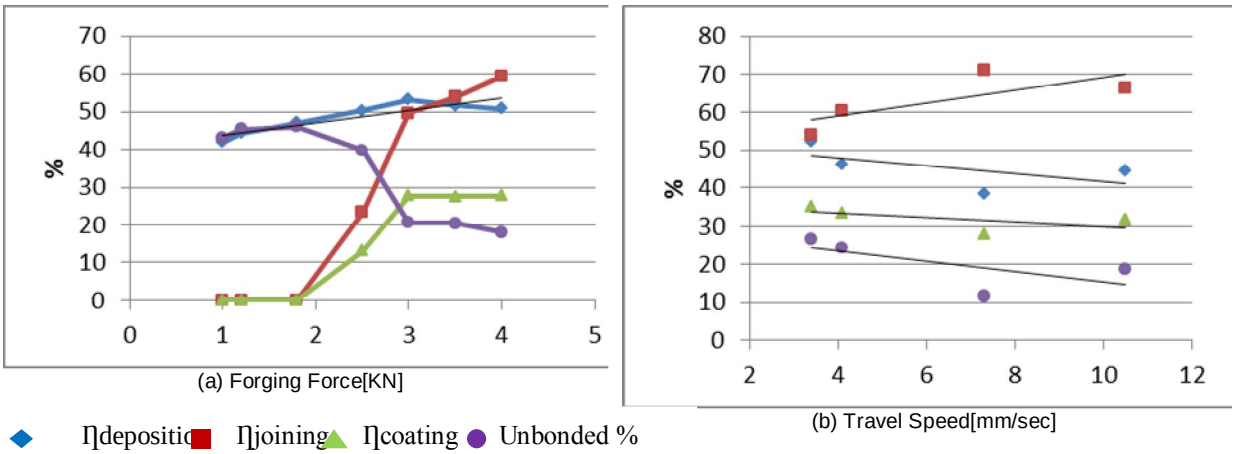

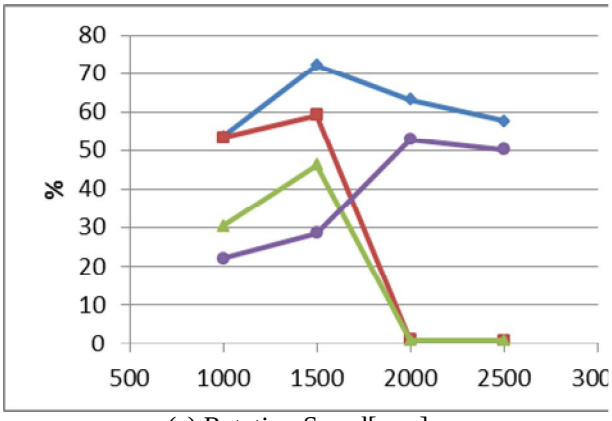

(c) Rotation Speed[rpm]

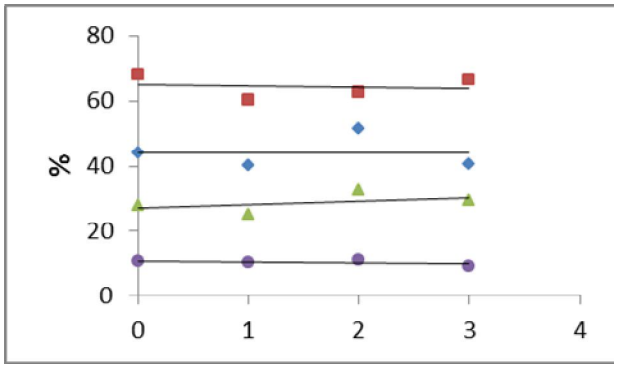

(d) Tilt Angle[degree]

Fig.8. Effect of process parameter on friction surfacing mass transfer efficiency. process parameters(a)Ω = 2000 rpm, γ=4.1 mm/sec (b) F= 3 KN, Ω = 2000 rpm(c) F= 2KN, γ=4.1 mm/sec (d) F= 3 KN, Ω = 2000 rpm, γ= 10.5 mm/sec

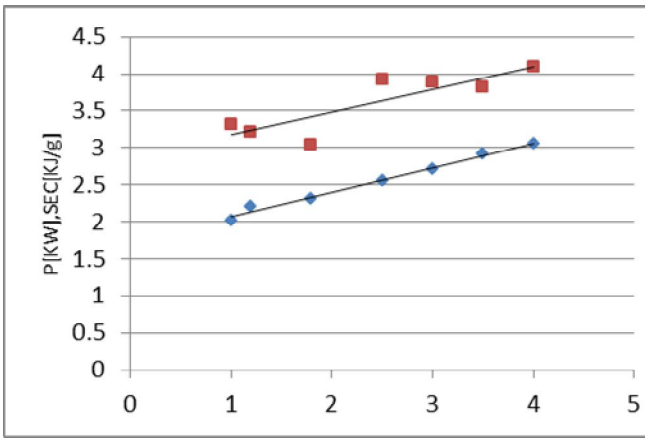

(a) Forging Force[KN]

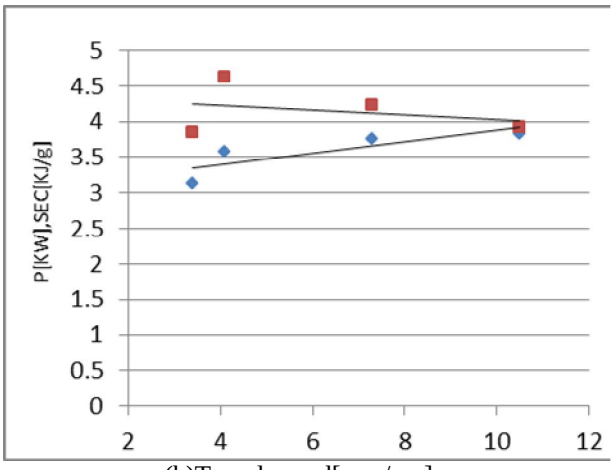

(b)Travel speed[mm/sec]

◆ p[kw], ■ SEC [KJ/g]

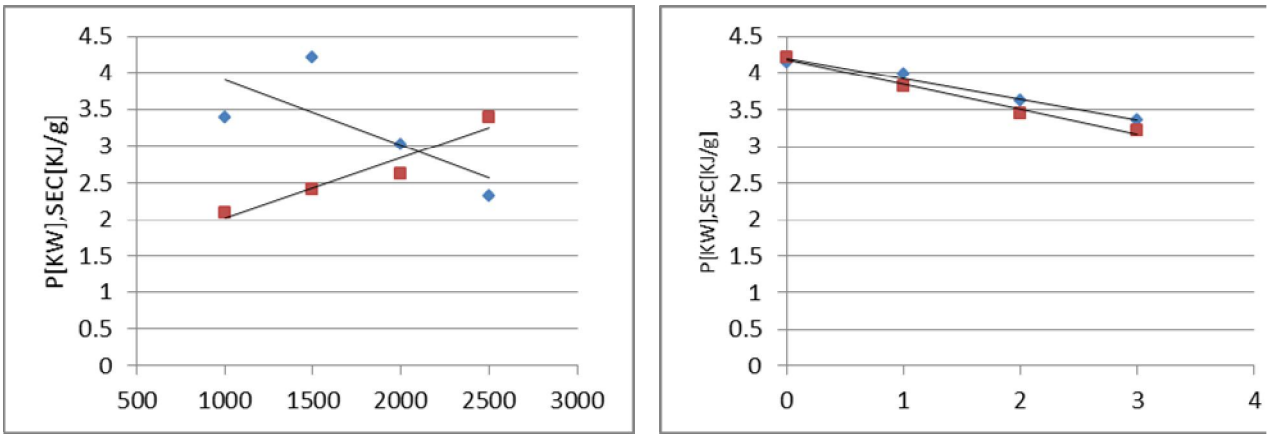

(c) Rotation Speed[rpm] (d) Tilt Angle[degree]

Fig.9. Effect of process parameter on friction surfacing power and specific energy consumption. process parameters(a)Ω = 2000 rpm, γ=4.1 mm/sec (b) F= 3 KN, Ω = 2000 rpm(c) F= 2KN, γ=4.1 mm/sec (d) F= 3 KN, Ω = 2000 rpm, γ= 10.5 mm/sec

VI. CONCLUSIONS

From the current work, the subsequent will be concluded:

• Friction surfacing allows intermediate mass deposition rates and higher energy efficiency in comparison with several mainstream laserbased and arcwelding cladding processes. It was seen to require mechanical work between 2.5 and 4 kJ/g of deposited coating with deposition rates of 0.5–1.5 g/s.

• Forging force enhances joining quality and coating hardness, while contributing to a better overall coating efficiency.• Faster travel speeds improve deposition rates and coating hardness, while decreasing energy consumption per unit of mass. Excessive travel speeds resulted in less connection potency.

• Excessive rotation speeds result in less joining efficiency and increased energy consumption per unit of mass.

• By adjusting a correct tilt angle, specific energy consumption drops, while slightly rising deposition rate and connection efficiency.

REFERENCES

[1] Batchelor, A.W., Jana, S., Koh, C.P., Tan, C.S., 1996. The effect of metal type and multilayering on friction surfacing. J. Mater. Process. Technol. 57, 172– 181.

[2] Dillip.J.J.S.,Babu.S.,Rajan.S.V.,Rafi.K.H.,Ram G.D.J., Stucker.B.E.,2013 Use of Friction Surfacing for additive Manufacturing,Materials Processing Technology 72(3),446-452

[3] Janakiraman.S.,Bhat.U.K., 2012. Formation of Composite during Friction Surfacing of Steel with Aluminium Advances in Tribology, Article ID 614278

[4] Chandrasekaran, M., Batchelor, A.W., Jana, S., 1997. Friction surfacing of metal coatings on steel and aluminum substrate. J. Mater. Process. Technol. 72, 446–452. Coherent Inc., 2011.

[5] Lachenicht, V., Scharf, G., Zebrowski, D., Shalimov, A., 2011. Spray forming – a promising process for making highquality steels and alloys. Metallurgist 54, 656–668.

[6] Macedo, M.L.K., Pinheiro, G.A., Santos, J.F., Strohaecker, T.R., 2010. Deposit by friction surfacing and its applications. Weld. Int. 24, 422–431.

[7] Rao.K.P.,Sreenu A.V.,Rafi.K.H.,Libin.M.N.,Balasubramaniam.K.,2012. Tool Steel nd copper coating by friction surfacing- A Thermgraphy tudy, Journal of Material processing Technology 212,402-407.

[8] Mishra, R.S., Ma, Z.Y., 2005. Friction stir welding and processing. Mater. Sci. Eng. R 50, 1–78.

[9] Nicholas, E.D., Thomas, W.M., 1986. Metal deposition by friction welding. Weld. J., 17–27.

[10] Rafi, H.K., Ram, G.D.J., Phanikumar, G., Rao, K.P., 2010. Friction surfaced tool steel (H13) coatings on low carbon steel: a study on the effects of process parameters on coating characteristics and integrity. Surf. Coat. Technol. 205, 232–242.

[11] Rafi, H.K., Ram, G.D.J., Phanikumar, G., Rao, K.P., 2011. Microstructural evolution during friction surfacing of tool steel H13. Mater. Des. 32, 82–87.

[12] Sauvage.X., Wetscher.F., Pareige.p.,2005 Mechanical alloying of Cu and Fe Induced by severe Plastic Deformtion of Cu-Fe Composite Acta Materialia 53,2127-2135

[13] Reddy, G.M., Rao, K.S., Mohandas, T., 2009. Friction surfacing: novel technique for metal matrix composite coating on aluminium–silicon alloy. Surf. Eng. 25, 25–30.
[14] Reddy, G.M., Prasad, K.S., Rao, K.S., Mohandas, T., 2011. Friction surfacing of titanium alloy with aluminium metal matrix composite. Surf. Eng. 27, 92–98.
[15] Vitanov, V.I., Voutchkov, I.I., Bedford, G.M., 2000. Decision support system to optimize the Frictec (friction surfacing) process. J. Mater. Process. Technol. 107, 236–242.
[16] Vitanov, V.I., Javaid, N., Stephenson, D.J., 2010. Application of response surface methodology for the optimisation of micro friction surfacing process. Surf. Coat. Technol. 204, 3501–3508.
[17] Vitanov, V.I., Voutchkov, I.I., 2005. Process parameters selection for friction surfacing applications using intelligent decision support. J. Mater. Process. Technol. 159, 27–32.